HHS Public Access

Author manuscript

AAPS J. Author manuscript; available in PMC 2018 June 18.

Published in final edited form as:

AAPS J. 2017 January ; 19(1): 141–149. doi:10.1208/s12248-016-9999-6.

Intra-articular Injection of Urinary Bladder Matrix Reduces Osteoarthritis Development

Heather N. Jacobs[1], **Sona Rathod**[1], **Matthew T. Wolf**[1], and **Jennifer H. Elisseeff**[1,2,3]

[1]Translational Tissue Engineering Center, Wilmer Eye Institute and Department of Biomedical Engineering, Johns Hopkins University, Baltimore, Maryland 21287, USA

[2]400N Broadway, Baltimore, Maryland 21232, USA

Abstract

Micronized porcine urinary bladder matrix (UBM) is an extracellular matrix biomaterial that has immunomodulatory and pro-regenerative properties. The objective of this study was to assess the ability of UBM to alter disease progression in a mouse model of post-traumatic osteoarthritis (OA). Ten-week-old wild-type C57BL/6 male mice underwent anterior cruciate ligament transection (ACLT) to induce OA. Two weeks after ACLT, UBM (50 mg/mL) or saline was injected into the mouse joint. At 4 and 8 weeks post-ACLT, cartilage integrity was assessed using OARSI scoring of histology, pain was evaluated, and joints were harvested for quantitative RT-PCR analysis of cartilage-specific and inflammatory gene expression. UBM-treated animals showed improved cartilage integrity at 4 and 8 weeks and reduced pain at 4 weeks compared to saline-injected mice. Animals injected with UBM expressed higher levels of genes encoding structural cartilage proteins, such as collagen2α1 and aggrecan, as well as anti-inflammatory cytokines, including interleukins 10 and 4. UBM decreased cartilage degeneration in the murine ACLT model of OA, which may be due to reduced inflammation in the joint and maintenance of high expression levels of proteoglycans.

Keywords

ACL transection; bioengineering; extracellular matrix; osteoarthritis; urinary bladder matrix

INTRODUCTION

Osteoarthritis (OA) is a prevalent degenerative musculoskeletal disease that results in both biological and mechanical dysfunction of the cartilage tissue that lines the surface of articulating joints. Between 2010 and 2012 alone, 52.5 million adults were diagnosed with OA in the USA (1). OA is characterized by a progressive loss of cartilage tissue, dysfunctional remodeling of the underlying bone, inflammation of the synovial membrane, and abnormalities in lubrication of the articular joint. Current therapies for OA are minimal and often palliative. Palliative options include non-steroidal anti-inflammatory drugs

[3]To whom correspondence should be addressed. (jhe@jhu.edu).

Electronic supplementary material The online version of this article (doi:10.1208/s12248-016-9999-6) contains supplementary material, which is available to authorized users.

(NSAIDs) and cortisone injections to control pain; however, these pharmaceuticals do not slow or reverse disease progression. The primary therapeutic treatment for OA is end-stage joint replacement, such as total-knee replacement surgery. These surgeries are invasive, and as severity of OA is increasing in younger patients, the comparably short lifetime of knee joint replacements present a challenge (2). The ultimate goal for OA treatment is to find a disease-modifying osteoarthritis drug (DMOAD) that can promote tissue regeneration, reduce or stop the progression of OA, and ultimately promote regeneration of the lost tissue. There is a small number of promising DMOAD pharmaceuticals currently in clinical development that aim to modulate either anabolism or catabolism of the cartilage tissue, or inhibit pro-inflammatory cytokine signaling. These therapies include intra-articular injection of an interleukin-1β (IL-1β) inhibitor and chondroitin sulfate (3). However, no DMOAD treatment has been approved by regulatory authorities due to lack of clinical efficacy (3).

Owing to the dearth of therapeutic options for OA, there remains a critical need for new approaches for treating disease and rebuilding tissue. Biomaterials-based strategies may be an option for degenerative musculoskeletal bone and cartilage diseases, as synthetic hydrogels have improved disease score in rabbits with post-traumatic OA (4) as well as in goats and humans with focal cartilage defects (5). Treatment with biologics composed of extracellular matrix (ECM) is a regenerative medicine option for tissue reconstruction.

Unlike synthetic polymeric materials, ECM scaffolds are composed of an intricate mixture of proteins, glycoproteins, and polysaccharides, which can be isolated by chemically and/ or mechanically removing cells from various tissue sources. The ECM provides structural support for cells, binds to and sequesters growth factors, and plays important roles in cell adhesion and signaling via integrins (6). These properties make the ECM a biologically active scaffold that influences cell differentiation, proliferation, survival, polarity, and migration (7). ECM scaffolds derived from different tissues have distinct properties, as the structure and function of each tissue is highly specific. For example, while cartilage tissue has a relatively low ratio of cells-to-ECM and high collagen and proteoglycan content, brain tissue contains a much higher ratio of cells-to-ECM, more secreted factors, and little collagen (8,9). The ECM can also be chemically and physically processed into several biomaterial configurations, including injectable particulates. ECM-derived materials manufactured from different tissues, such as urinary bladder and small intestinal submucosa, have applications ranging from burn wound treatment to urinary tract repair (10). Additionally, ECM has been used in a small animal model of post-traumatic OA to reduce cartilage degeneration (11).

In this study, we are using particulate ECM as a biologic and immunomodulatory agent to advance OA therapy and cartilage tissue regeneration. We investigated an ECM biomaterial derived from porcine urinary bladder matrix (UBM), which maintains an intact basement membrane with high amount of collagens III and VII (12), elastic fibers, adhesive proteins, and glycoproteins (12). UBM has been shown to promote regeneration in soft tissue injury through a number of mechanisms. Remodeling UBM was shown to shift the local macrophage response *in vivo* towards a pro-healing, anti-inflammatory phenotype (13), and recruits progenitor cell proliferation and differentiation after traumatic muscle injury in mice (14). UBM similarly promoted muscle repair in patients with volumetric muscle loss in a

clinical study (15). UBM has also been applied clinically to chronic non-healing ulcers and has resulted in epithelialization of the ulcers with limited scar tissue formation (16,17). Additionally, UBM was applied to complicated wounds not responding to conventional therapies with the result of epithelialization and successful skin grafting (18). UBM also facilitates soft tissue reconstruction in traumatic wounds by establishing a neovascularized soft tissue base (19).

The physicochemical and immunomodulatory properties of UBM make it an attractive therapeutic for OA, as OA—previously regarded as a predominantly mechanical disease—is now thought to progress due to excessive inflammation, immune cell infiltration, and cytokine secretion (20–22). Only one other report has shown the use of ECM in a small animal model of post-traumatic OA, but used human amnion ECM and has not shown evidence of the mechanism by which ECM helped reduce cartilage degeneration or shown functional pain reduction (11). We therefore tested the effect of UBM on OA disease progression and tissue regeneration in rodents by injecting micronized UBM into a mouse model of post-traumatic OA, and by treating primary human chondrocyte cultures from OA cartilage *in vitro*. The results indicate a positive effect of UBM treatment on cartilage integrity *in vivo*, improved functional outcomes, and enhanced expression of several structural cartilage and anti-inflammatory genes.

METHODS

Surgical Procedures

All procedures were approved by the Johns Hopkins University Animal Care and Use Committee (ACUC). OA was induced by anterior cruciate ligament transection (ACLT) (23) in 10-week-old male C57BL/6 mice from Charles River. Two weeks after ACLT, a single 10-μL injection of either a phosphate-buffered saline (1× PBS, from Life Technologies) vehicle control or micronized UBM (~88% of the particle volume was under 20 μm and the D50 (median size) was 5.09 μm) suspended in 1× PBS, pH 7.2, 50 mg/mL, from ACell®, Inc., Columbia, MD was administered to the joint space of the operated knee via a 30-gauge needle (n = 13 animals for 4-week, n = 8 animals for 8-week time point). The joint cavity was opened in the sham group but the ACL was not transected. The study design is depicted in Fig. 1a. UBM particles were made using a Retsch CryoMill from Verder Scientific. A single steel ball (25 mm diameter) resides with the raw UBM sheet material during grinding. The chamber was kept cool via liquid nitrogen. Data on particle size distribution is in supplementary Fig. S2.

Histological evaluation

After 4 or 8 weeks, animals were sacrificed and mouse knees were fixed in 4% paraformaldehyde (PFA), decalcified for approximately 2 weeks in 10% EDTA, then dehydrated and embedded in paraffin. Seven-micrometer-thick sections were taken throughout the joint and stained for proteoglycans with Safranin-O and Fast Green (Applied biosciences) per manufacturer's instructions. Osteoarthritis Research Society International (OARSI) scores are based on blinded histological assessment the medial plateau of the tibia (24).

Immunohistochemistry

Slides were de-paraffinized and treated with hyaluronidase (0.25% in Tris buffer) before staining for COL2 using Anti-Collagen II antibody (ab34712) from Abcam at 1:300 dilution (in 4% BSA/0.25% Triton X-100) followed by secondary staining with a biotinylated antibody and streptavidin-peroxidase conjugated enzyme using the Histostain-SP IHC kit, AEC, from ThermoFisher (cat. no. 959943) according to the manufacturer's instructions.

Gene Expression Analysis

Whole mouse joints were frozen in liquid nitrogen and homogenized using a sterile mortar and pestle. RNA was extracted using TRIzol reagent (Life Technologies) following the manufacturer's protocol. cDNA was synthesized using Superscript III reverse transcriptase (Life Technologies) following the manufacturer's protocol. Real-time RT-PCR was carried out using SYBR Green primers and a StepOnePlus Real-time PCR System (Life Technologies). Relative gene expression was calculated by the ΔΔCt method. The ΔCt was calculated using the reference genes β2-microglobulin (*B2m*) and β-actin (*Bact*). ΔΔCt was calculated relative to the un-operated control group. The mouse specific primers used were the following: *Bact* forward, CCA CCG TGA AAA GAT GAC CC, *Bact* reverse, GTA GAT GGG CAC AGT GTG GG, *B2m* forward, CTC GGT GAC CCT GGT CTT TC, *B2m* reverse, GGA TTT CAA TGT GAG GCG GG, *Acan* forward, CGT TGC AGA CCA GGA GCA AT, *Acan* reverse, CGG TCA TGA AAG TGG CGG TA, *Col2a1* forward, CCT CCG TCT ACT GTC CAC TGA, *Col2a1* reverse, ATT GGA GCC CTG GAT GAG CA, *Mmp13* forward, GTC TTC ATC GCC TGG ACC ATA, *Mmp13* reverse, GGA GCC CTG ATG TTT CCC AT, *Runx2* forward, GCC GGG AAT GAT GAG AAC TA, *Runx2* reverse, GGT GAA ACT CTT GCC TCG TC, *Il4* forward, ACA GGA GAA GGG ACG CCA T, *Il4* reverse, ACC TTG GAA GCC CTA CAG A, *Il10* forward, TCT CAC CCA GGG AAT TCA AA, *Il10* reverse, AAG TGA TGC CCC AGG CA, *Il6* forward, CCA GGT AGC TAT GGT ACT CCA GAA, *Il6* reverse, GCT ACC AAA CTG GAT ATA ATC AGG A, *IL1b* forward, GTA TGG GCT GGA CTG TTT C, *IL1b* reverse, GCT GTC TGC TCA TTC ACG.

Hind Limb Weight-Bearing Assessment

Weight-bearing in mice was measured in the un-operated control animals and compared to ACLT animals receiving PBS control or UBM therapy using an incapacitance tester (Columbus Instruments). The percentage weight distributed on the ACLT limb was used as an index of joint discomfort in OA (23). The mice were positioned to stand on their hind paws in an angled box placed above the incapacitance tester so that each hind paw rested on a separate force plate. The force (g) exerted by each limb was measured. Three consecutive 3-s readings were taken and averaged to obtain the mean score (25).

Hind Limb Responsiveness

Mice were placed on the hotplate at 55°C. The latency period for hind limb response (jumping or paw-lick) was recorded as response time before surgery and at 2 and 4 weeks after surgery in all animal groups (23). Three readings were taken per mouse and averaged to obtain the mean response time for each time point.

Human Chondrocyte Isolation and Cell Culture

Human chondrocytes were isolated from OA cartilage harvested from cadaveric sources (n = 3) from the National Disease Research Interchange. Cartilage was minced to 1-mm^3 pieces, rinsed 3× in 1× PBS, and suspended in 25 mL of collagenase media [DMEM with 5% FBS and 1.67 mg/mL type II collagenase] per every 10 mL of cartilage pieces, then placed on a shaker at 37°C for 16–18 h. Cells were filtered through a 70-μm cell strainer, spun down at 1000 rpm for 10 min, and rinsed 3× with PBS. Chondrocytes were plated in a six-well plate with ~250,000 cells/well in chondrocyte media (high-glucose DMEM supplemented with 10% FBS, 1% nonessential amino acids, 1% HEPES, 1% sodium pyruvate, 0.2 M L-proline, 25 mg/mL ascorbic acid, and 1% pen/strep). After ~4 h of attachment, 10 ng/mL of IL-1β was added to the media and allowed to incubate for 16–18 h before addition of UBM, which then incubated for 24 h before cell isolation for PCR. ΔΔCt was calculated relative to the untreated control group that received only IL-1β. The following human specific primers were used: *BACT* forward, GCT CCT CCT GAG CGC AAG TAC, *BACT* reverse, GGA CTC GTC ATA CTC CTG CTT GC, *B2M* forward, GAG GCT ATC CAG CGT ACT CCA, *B2M* reverse, CGG CAG GCA TAC TCA TCT TTT, *MMP13* forward, TGG TCC AGG AGA TGA AGA CC, *MMP13* reverse, TCC TCG GAG ACT GGT AAT GG, *ADAMTS5* forward, GAG GCC AAA AAT GGC TAT CA, *ADAMTS5* reverse, GGC AGG ACA CCT GCA TAT TT, *NF-kB* forward, AAC AGA GAG GAT TTC GTT TCC G, *NF-kB* reverse, TTT GAC CTG AGG GTA AGA CTT CT, *TNFα* forward, CCT CTC TCT AAT CAG CCC TCT G, *TNFα* reverse, GAG GAC CTG GGA GTA GAT GAG, *IL6* forward, GGC ACT GGC AGA AAA CAA CC, *IL6* reverse, GCA AGT CTC CTC ATT GAA TCC, *IL1β* forward, GGA CAA GCT GAG GAA GAT GC, *IL1β* reverse, TCG TTA TCC CAT GTG TCG AA.

Alamar Blue Assay

Human OA chondrocytes were plated at a density of 10,000 cells/well in a 96-well plate and incubated at 37°C until attachment occurred, after which 10 ng/ mL of IL-1β and varying concentrations of UBM were added to the media and allowed to incubate for 24 h. Ten microliters of Alamar Blue® reagent (ThermoFisher Scientific) was added directly into each well and the plate was incubated at 37°C for 3 h protected from light. Absorbance was measured using a microplate reader every hour for 3 h at a wavelength of 570 nm. Data were normalized to readings at 600 nm. These measurements were used to calculate percent of Alamar Blue reduced compared to control (cells with IL-1β but no UBM).

UBM Particle Labeling and Confocal Microscopy

UBM particles were suspended in bicarbonate buffer (pH = 8.3) and labeled with an Alexa Fluor-488 N-hydroxysuccinimide ester conjugate (Thermo Fisher) for 2 h at room temperature. Excess dye was removed by washing several times with PBS via centrifugation. Fluorescent labeling and dye removal was confirmed by fluorescence measurements with a plate reader (BioTek Synergy 2). Labeled and unlabeled particles were added to human chondrocytes cultured on 1.5 mm thickness coverglass chamber wells (ThermoFisher Scientific) for 24 h. Cells were then washed with PBS to remove unbound ECM and fixed with 4% paraformaldehyde for 20 min at room temperature. Cell membranes and nuclei

were counterstained the CellMask Deep Red plasma membrane stain (Thermo) and DAPI, respectively, for 5 min. Entire cell volumes were imaged using a Zeiss LSM 710 confocal microscope with a ×63 oil immersion objective and 0.3 μm slice thickness. Three-dimensional cell reconstruction was performed using IMARIS software (Bitplane).

Statistical Analysis

Statistical analysis was performed using a one-way ANOVA with Holm-Sidak multiple comparison correction in GraphPad Prism Software. For *in vivo* work, all groups were compared to each other. For *in vitro* work, each treatment was compared to the control group. $p < 0.05$ was considered significant.

RESULTS

UBM Injection Reduces OA Progression in Mice

The ACLT model of post-traumatic OA was chosen for its reproducibility and its relevance to human injury; approximately 50% of people of who tear their ACL develop OA within 10–20 years (26). The mouse ACLT model develops OA about 4 weeks after injury (27). ACL-transected mouse knees were injected with UBM particles or saline at 2 weeks post-ACLT and the effects on cartilage integrity and whole joint inflammation were assessed at 4 and 8 weeks (2 and 6 weeks after therapy, respectively) (Fig. 1a). OARSI scoring, which is indicative of OA severity on a scale of 0 to 5 (0 is no cartilage degeneration, 5 is severe degeneration) revealed a statistically significant decrease in OA severity following UBM treatment group compared to saline controls at both 4 and 8 weeks. UBM particles reduced average disease scores from 3.2 to 1.4 at 4 weeks and from 3.7 to 1.9 at 8 weeks compared to saline alone (Fig. 1b). At 4 weeks, mice treated with the saline control exhibited proteoglycan loss as shown by diminished safranin-o staining (Fig. 1c; arrows) and cartilage lesions (Fig. 1c; stars) on their tibia. Injection of UBM in the synovial cavity decreased the severity of lesions and qualitatively increased the proteoglycan staining compared to the saline control (Fig. 1c). This effect was maintained even at 8 weeks post-injury, indicating a protective effect of UBM treatment on cartilage structure.

UBM Therapy Decreases Expression of Inflammatory Markers

We next sought to characterize the osteoarthritic microenvironment after UBM treatment. As OA is a whole joint disease involving the cartilage and synovial tissue, inflammatory gene expression was evaluated in whole knee joint tissue using qRT-PCR. Cytokines thought to be involved in the pathophysiology of OA are the pro-inflammatory cytokines IL-1β, tumor necrosis factor α (TNF-α), and IL-6, which increase the production of matrix metalloprotease 13 (MMP-13), a collagenase that participates in cartilage degeneration (26). Macrophages are hypothesized to be important in OA and contribute to the expression of these cytokines; M1 polarized macrophages produce the pro-inflammatory cytokines IL-1β, IL-6, and IFNγ (28), whereas M2 polarized macrophages often produce the anti-inflammatory cytokines IL-10, IL-4, and IL-13.

Gene expression of these inflammatory cytokines as well as cartilage catabolism and anabolism were evaluated in whole mouse joints at 4 and 8 weeks post-ACLT (Fig. 2). At 4

weeks, joints treated with UBM demonstrated significantly increased expression of the structural genes Aggrecan (*Acan*, approximately 9-fold) and collagen 2α1 (*Col2a1*, 13-fold) in addition to the anti-inflammatory genes *Il4* (2.6-fold) and *Il10* (5-fold) over un-operated control when compared to the saline control, which did not affect expression (Fig. 2a, b). Additionally, the 4-week UBM treatment group reduced expression of the inflammatory cytokine *Il1b* compared to saline injections with 1.4- and 2.5-fold changes from un-operated mice, respectively. Conversely, expression of the pro-inflammatory cytokine *Il6* and enzyme *Mmp13* was increased in the saline group as compared to un-operated wild-type mice (3-fold and 5-fold, respectively), but not in the UBM group. Runx2 expression was not affected by any treatment suggesting that there was no chondrocyte hypertrophy. This is consistent with the observed increase in ECM gene expression as chondrocyte hypertrophy is associated with negative cartilage remodeling, including decreased collagen and proteoglycan production and alkaline phosphatase secretion, allowing abnormal calcification of the articular cartilage to occur.

At 8 weeks, joints treated with UBM demonstrated significantly increased expression of the anti-inflammatory gene *Il10* (3.8-fold) compared to the saline control (no change) (Fig. 3). Aggrecan (*Acan*) also exhibited significantly increased expression in the UBM-treated group compared to an age-matched normal control (2.2-fold). No other genes were affected by UBM injection, indicating that the anti-inflammatory effect of the UBM had resolved between 4 and 8 weeks post-ACLT (Fig. 3). The maintenance of cartilage integrity observed at 8 weeks post-ACLT and the sustained increase in *Il10* and *Acan* expression suggests that the therapeutic effects of UBM may be mediated, at least in part, by these genes.

To validate the finding of increased collagen 2α1 expression in UBM-treated mice, histological sections from each treatment group were stained for the collagen 2α1 protein (COL2α1) (Fig. 4). Cartilage from UBM-treated mice at 4 weeks consistently stained more intensely for COL2α1 than the saline control cartilage. The 8-week UBM treatment group stained more intensely than the 8-week saline control despite not expressing significantly higher *Col2a1* (as assayed by qPCR) (Fig. 3). This discrepancy could be due to the fact that collagen protein can be retained long after *Col2a1* gene expression has diminished.

UBM Injection Reduces Pain in OA Mice

After the majority of intra-articular cartilage is damaged from OA, severe pain arises from exposed nerve endings that were once protected by the dense cartilage. This is a hallmark of OA and can serve as a clinical endpoint for treatment trials. Thus, we determined if the UBM-mediated improvement in cartilage structure (shown in Fig. 1a) correlated with a functional decrease in pain through hotplate and incapacitance testing (Fig. 5) (23). The UBM-treated groups at 4 and 8 weeks exhibited faster response time with the hotplate test, on par with the healthy sham animals, which indicates decreased motor impairments compared to saline-injected mice (Fig. 5a). UBM-treated animals also demonstrated greater weight-bearing percentage on the operated limb at 4 weeks, indicating less functional impairment than saline-treated mice despite ACLT (Fig. 5b). At 8 weeks, however, weight-bearing percentage was not statistically different between the control (saline) group and UBM-treated animals.

UBM Decreased Inflammatory Marker Expression in Human OA Chondrocytes

Pro-regenerative gene expression within the mouse knee after UBM treatment led us to ask whether there was a biological effect of UBM on human OA chondrocytes. 2D culture is not a perfect model of what occurs in the knee joint; however, *in vitro* chondrocyte culture has been used to elucidate biological effects of therapeutics (25).

To maintain OA conditions *in vitro*, primary human OA chondrocytes were cultured in the presence of IL-1β for 1 day prior to the addition of varying concentrations of UBM. We assessed the expression of several genes involved in OA progression after 1 day of UBM exposure. Genes tested included the matrix-degrading enzyme *MMP13*, the pro-inflammatory stress-related transcription factor *NF-κB1* (nuclear factor kappa-light-chain-enhancer of activated B cells), the aggrecan-degrading enzyme *ADAMTS5* (a disintegrin and metalloproteinase with thrombospondin motifs 5), and the pro-inflammatory cytokines *TNFα*, *IL6*, and *IL1β*. As chondrocytes are the cell type synthesizing aggrecan, a major structural component of cartilage, it is relevant to observe expression of *ADAMTS5*, the enzyme that degrades aggrecan. UBM induced a dose-dependent response in most genes tested. The 100 and 1000 ng/mL concentrations of UBM produced the most apparent reductions in inflammatory cytokine and matrix-degrading enzyme expression, while the lowest concentrations (1, 10 ng/mL) had no beneficial effects (Fig. 6). The 1 μg/mL UBM dose lowered *MMP13* compared to the control group (0.5-fold). There was also a trend of reduced *NF-κB1* and *ADAMTS5* expression by UBM treatment (by 0.4- and 0.6-fold, respectively), but did not reach statistical significance ($p = 0.054$, 0.07, respectively). This trend of decreased inflammatory cytokine and matrix-degrading enzyme expression is similar to our findings *in vivo*. Additionally, the Alamar Blue assay was performed to confirm that UBM treatment is not toxic. There were no significant changes in percent reduction of Alamar Blue across the tested UBM concentrations.

To determine how UBM may be directly interacting with chondrocytes *in vitro*, confocal imaging was performed 24 h after adding 1 μg/mL or 100 μg/mL of fluorescently labeled UBM to chondrocyte media. Imaging revealed that human chondrocytes do not engulf UBM entirely, but do appear to contact the surface of most particles (Fig. 6b).

DISCUSSION

ECM biomaterials, such as UBM, are an attractive therapy for OA disease modification due to their regenerative capabilities in animal models and in humans (11,15). UBM is used clinically for several different applications including management of trauma wounds (29), chronic non-healing wounds (2), and esophageal reinforcement in gastrectomy (7). Because OA does not yet have a viable treatment, and UBM has shown promise in other musculoskeletal defects and degenerative diseases, the possibility of UBM to treat OA was tested here in a mouse model and in human primary cells. Injection of UBM into the synovial cavity of mice with ACLT-induced OA improved the articular cartilage integrity 4 and 8 weeks after injury and reduced pain compared to saline-treated controls. At 4 weeks, the expression of structural genes (*Acan*, *Col2α1*) and anti-inflammatory cytokines (*IL4*, *IL10*) was significantly increased compared to controls. Accordingly, UBM treatment decreased the expression of the pro-inflammatory cytokine *Il1β in vivo* in mice and the

remodeling enzyme *MMP-13 in vitro* in human OA chondrocytes. While chondrocytes exhibited reduced expression of matrix-degrading and pro-inflammatory genes, it is unclear to what extent particles would interact with them directly. Alternatively, the synovium is more permeable to particle passage meaning that synoviocytes may be more likely to encounter particles in synovial fluid; their response to UBM is worthy of further investigation (30).

These results are consistent with the theorized role of the immune response in OA disease progression. Previously, Finnegan *et al.* described a role of IL-10, an important anti-inflammatory cytokine, in collagen-induced arthritis. The severity of arthritis in IL-10 knockout ($Il10^{-/-}$) mice was substantially greater than that in wild-type or $Il10^{+/-}$ (heterozygous) mice, indicating a role for IL-10 in moderating disease severity (31). In a separate study on rabbits with OA, IL-10 cDNA delivered *ex vivo* to rabbit synoviocytes and then injected intra-articularly was able to reduce cartilage breakdown (32). These reports are consistent with our findings of IL-4 and IL-10 expression accompanied by cartilage protection.

The observed high expression of type II collagen and proteoglycan genes is most likely beneficial in maintaining cartilage integrity (25). Tesche *et al.* found that type II collagen was synthesized by the remaining healthy chondrocytes in OA, but not by the fibroblast-like chondrocytes that produce an abnormal matrix (33,34). Salminen *et al.* noted that articular chondrocytes are capable of producing type 2A procollagen, but near the margins of cartilage defects, chondrocytes were metabolically inactive and surrounded by a noncollagenous matrix, which probably contributed to the loss of cartilage integrity (35). These findings point to a dynamic in which proteoglycan expression occurs in OA and may actually help maintain cartilage integrity; it is only when collagenases and aggrecanases exceed this repair capability that the cartilage shifts to production of an abnormal matrix, leading to a loss of cartilage integrity resulting in a defect. Because inflammatory cytokines encourage the expression of catabolic enzymes, perhaps control of the inflammation in the knee using biomaterials such as UBM may help shift the balance in the favor of anabolic genes and maintain the cartilage integrity. UBM may additionally work by directly encouraging deposition of chondrocyte-derived matrix; ECM materials are known to induce deposition of host-derived matrix after being degraded by the host (3). Enhanced matrix deposition by UBM was supported in the mouse joints by increased *Col2a1* and *Acan* expression at the 4 weeks time point. At the 8 week UBM treatment time point, it is plausible that collagen protein was retained well after gene expression had diminished.

In our study, the heightened expression of *Il-10* and *Il-4* suggests that there may be type-2 immune cells (M2 macrophages and Th2 T cells) infiltrating the joint at higher numbers in the UBM-treated animals than in saline controls. M1 macrophages and Th1 T cells are known to lead to type 1, pro-inflammatory immune response (28) while M2 macrophages and Th2 T cells are anti-inflammatory and can lead to matrix deposition (36). Because the dysregulation of these cell types leads to immune-mediated pathologies, it is reasonable that balancing these cell types can help modify OA disease progression (36). Future studies may elucidate how immune cell populations change over the course of OA and how they change with UBM therapy. Additionally, gene expression of these separate cell populations can be

examined to identify which immune cell populations are responsible for the increases in IL-4 and IL-10 expression.

In conclusion, injection of UBM in the intra-articular space lessens cartilage degeneration in an ACLT mouse model of OA, and also induces a dose-dependent pro-regenerative, anti-inflammatory gene expression profile in human OA chondrocytes. This therapeutic effect may be due to the reduced inflammation in the joint and maintenance of high expression levels of proteoglycans, which together help to retain normal cartilage and limit tissue degradation. To further validate the use of UBM as an OA therapeutic, additional animal models should be tested (37). Today, there are no FDA-approved disease-modifying OA drugs available, making comparisons of UBM to current therapeutic options difficult. However, reduction in OA-associated pain could be compared to NSAIDs, viscosupplements, or biological injections such as platelet-rich plasma (PRP) (37,38).

Supplementary Material

Refer to Web version on PubMed Central for supplementary material.

Acknowledgments

The authors would like to thank M. Frisk for editing, Okhee Jeon for histology scoring, The Wilmer NEI-NIH funded Imaging Core, the Wilmer Pooled Professor Fund, and Rhonda Grebe for confocal expertise. ACell Inc. for supplying UBM and providing financial support for the study through a Sponsored Research Agreement was also acknowledged.

References

1. Centers for Disease Control and Prevention (CDC). Prevalence of doctor-diagnosed arthritis and arthritis-attributable activity limitation—United States, 2010–2012. MMWR Morb Mortal Wkly Rep. 2013; 62(44):869–73. [PubMed: 24196662]
2. Sutton PM, Holloway ES. The young osteoarthritic knee: dilemmas in management. BMC Med. 2013; 11:14. [PubMed: 23331908]
3. Martel-Pelletier J, Wildi LM, Pelletier JP. Future therapeutics for osteoarthritis. Bone. 2012; 51(2): 297–311. [PubMed: 22037003]
4. Oprenyeszk F, et al. Protective effect of a new biomaterial against the development of experimental osteoarthritis lesions in rabbit: a pilot study evaluating the intra-articular injection of alginate-chitosan beads dispersed in an hydrogel. Osteoarthr Cartil. 2013; 21(8):1099–107. [PubMed: 23680875]
5. Sharma B, et al. Human cartilage repair with a photoreactive adhesive-hydrogel composite. Sci Transl Med. 2013; 5(167):167ra6.
6. Gao Y, et al. The ECM-cell interaction of cartilage extracellular matrix on chondrocytes. Biomed Res Int. 2014; 2014:648459. [PubMed: 24959581]
7. Hynes RO. The extracellular matrix: not just pretty fibrils. Science. 2009; 326(5957):1216–9. [PubMed: 19965464]
8. Beachley VZ, et al. Tissue matrix arrays for high-throughput screening and systems analysis of cell function. Nat Methods. 2015; 12(12):1197–204. [PubMed: 26480475]
9. Wilson, J., Hunt, T. Molecular biology of the cell: a problems approach. 4. New York: Garland Science; 2002. p. xxiip. 711
10. Badylak SF. Regenerative medicine and developmental biology: the role of the extracellular matrix. Anat Rec B New Anat. 2005; 287(1):36–41. [PubMed: 16308858]

11. Willett NJ, et al. Intra-articular injection of micronized dehydrated human amnion/chorion membrane attenuates osteoarthritis development. Arthritis Res Ther. 2014; 16(1):R47. [PubMed: 24499554]
12. Brown B, et al. The basement membrane component of biologic scaffolds derived from extracellular matrix. Tissue Eng. 2006; 12(3):519–26. [PubMed: 16579685]
13. Wolf MT, et al. Macrophage polarization in response to ECM coated polypropylene mesh. Biomaterials. 2014; 35(25):6838–49. [PubMed: 24856104]
14. Song J. Porcine urinary bladder extracellular matrix activates skeletal myogenesis in mouse muscle cryoinjury. J Tissue Eng Regen Med. 2014; 3:3.
15. Sicari BM, et al. An acellular biologic scaffold promotes skeletal muscle formation in mice and humans with volumetric muscle loss. Sci Transl Med. 2014; 6(234):234ra58.
16. Kimmel H, Rahn M, Gilbert TW. The clinical effectiveness in wound healing with extracellular matrix derived from porcine urinary bladder matrix: a case series on severe chronic wounds. J Am Col Certif Wound Spec. 2010; 2(3):55–9. [PubMed: 24527148]
17. Lecheminant J, Field C. Porcine urinary bladder matrix: a retrospective study and establishment of protocol. J Wound Care. 2012; 21(10):476, 478–80, 482. [PubMed: 23103481]
18. Parcells A. The use of urinary bladder matrix in the treatment of complicated open wounds. Wounds. 2014; 26(7):189–96. [PubMed: 25860538]
19. Valerio I. The use of urinary bladder matrix in the treatment of trauma and combat casualty wound care. Regen Med. 2015; 10(5):611–22. [PubMed: 26237704]
20. Benito MJ, et al. Synovial tissue inflammation in early and late osteoarthritis. Ann Rheum Dis. 2005; 64(9):1263–7. [PubMed: 15731292]
21. Revell PA, et al. The synovial membrane in osteoarthritis: a histological study including the characterisation of the cellular infiltrate present in inflammatory osteoarthritis using monoclonal antibodies. Ann Rheum Dis. 1988; 47(4):300–7. [PubMed: 3259125]
22. de Lange-Brokaar BJ, et al. Synovial inflammation, immune cells and their cytokines in osteoarthritis: a review. Osteoarthr Cartil. 2012; 20(12):1484–99. [PubMed: 22960092]
23. Ruan MZ, et al. Pain, motor and gait assessment of murine osteoarthritis in a cruciate ligament transection model. Osteoarthr Cartil. 2013; 21(9):1355–64. [PubMed: 23973150]
24. Glasson SS, et al. The OARSI histopathology initiative—recommendations for histological assessments of osteoarthritis in the mouse. Osteoarthr Cartil. 2010; 18(Suppl 3):S17–23.
25. Ruan MZ, et al. Proteoglycan 4 expression protects against the development of osteoarthritis. Sci Transl Med. 2013; 5(176):176ra34.
26. Kapoor M, et al. Role of proinflammatory cytokines in the pathophysiology of osteoarthritis. Nat Rev Rheumatol. 2011; 7(1):33–42. [PubMed: 21119608]
27. Kamekura S, et al. Osteoarthritis development in novel experimental mouse models induced by knee joint instability. Osteoarthr Cartil. 2005; 13(7):632–41. [PubMed: 15896985]
28. Ferrante CJ, Leibovich SJ. Regulation of macrophage polarization and wound healing. Adv Wound Care. 2012; 1(1):10–6.
29. Boehler RM, Graham JG, Shea LD. Tissue engineering tools for modulation of the immune response. Biotechniques. 2011; 51(4):239–40. 242, 244 passim. [PubMed: 21988690]
30. Evans CD. The wear particles of synovial fluid: their ferrographic analysis and pathophysiological significance. Technical Notes. 1981
31. Finnegan A, et al. Collagen-induced arthritis is exacerbated in IL-10-deficient mice. Arthritis Res Ther. 2003; 5(1):R18–24. [PubMed: 12716449]
32. Zhang X. Suppression of early experimental osteoarthritis by gene transfer of interleukin-1 receptor antagonist and interleukin-10. J Orthop Res. 2006; 22:4.
33. Miosge N, et al. Expression of collagen type I and type II in consecutive stages of human osteoarthritis. Histochem Cell Biol. 2004; 122(3):229–36. [PubMed: 15316793]
34. Tidball JG, Villalta SA. Regulatory interactions between muscle and the immune system during muscle regeneration. Am J Physiol Regul Integr Comp Physiol. 2010; 298(5):R1173–87. [PubMed: 20219869]

35. Salminen H, Vuorio E, Saamanen AM. Expression of Sox9 and type IIA procollagen during attempted repair of articular cartilage damage in a transgenic mouse model of osteoarthritis. Arthritis Rheum. 2001; 44(4):947–55. [PubMed: 11315934]

36. Martinez FO, Gordon S. The M1 and M2 paradigm of macrophage activation: time for reassessment. F1000Prime Rep. 2014; 6:13. [PubMed: 24669294]

37. Poole R, et al. Recommendations for the use of preclinical models in the study and treatment of osteoarthritis. Osteoarthr Cartil. 2010; 18(Suppl 3):S10–6. [PubMed: 20864015]

38. da Costa BR, et al. Effectiveness of non-steroidal anti-inflammatory drugs for the treatment of pain in knee and hip osteoarthritis: a network meta-analysis. Lancet. 2016; 387(10033):2093–105. [PubMed: 26997557]

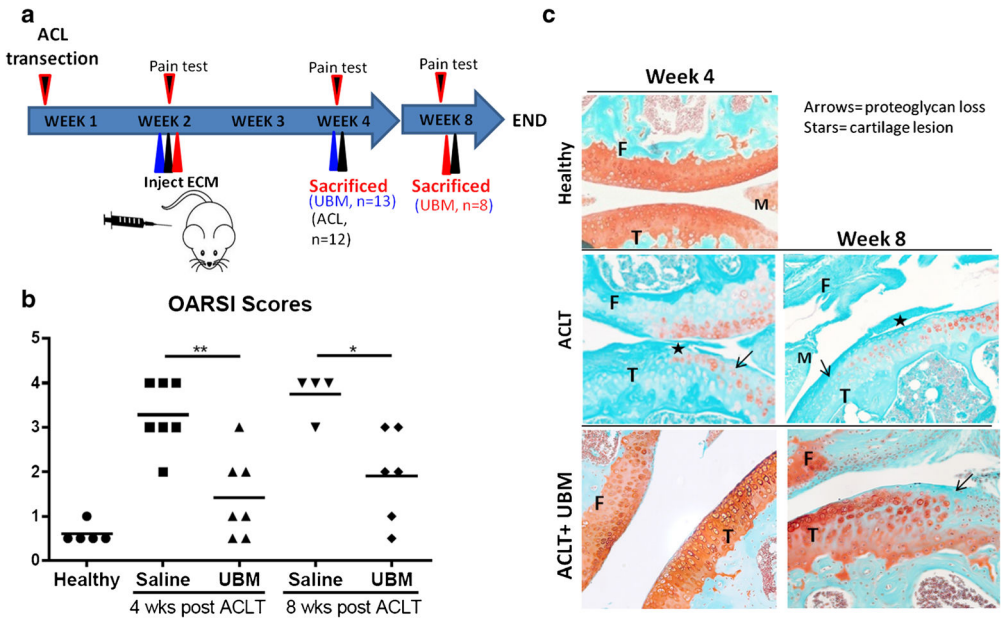

Fig. 1.

UBM-treated mice show reduced OA progression. **a** Overview of treatment. Mice were injected with 50 mg/mL of UBM (10–20 μm particles) 2 weeks after ACL transection and euthanized at 4 and 8 weeks post ACL transection. **b** OARSI scores from the medial plateau of each animal. *$p < 0.05$, **$p < 0.01$, ***$p < 0.001$. **c** Representative images from each treatment group, Safranin-O stained. *Arrows* = proteoglycan loss. *Stars* = cartilage lesion

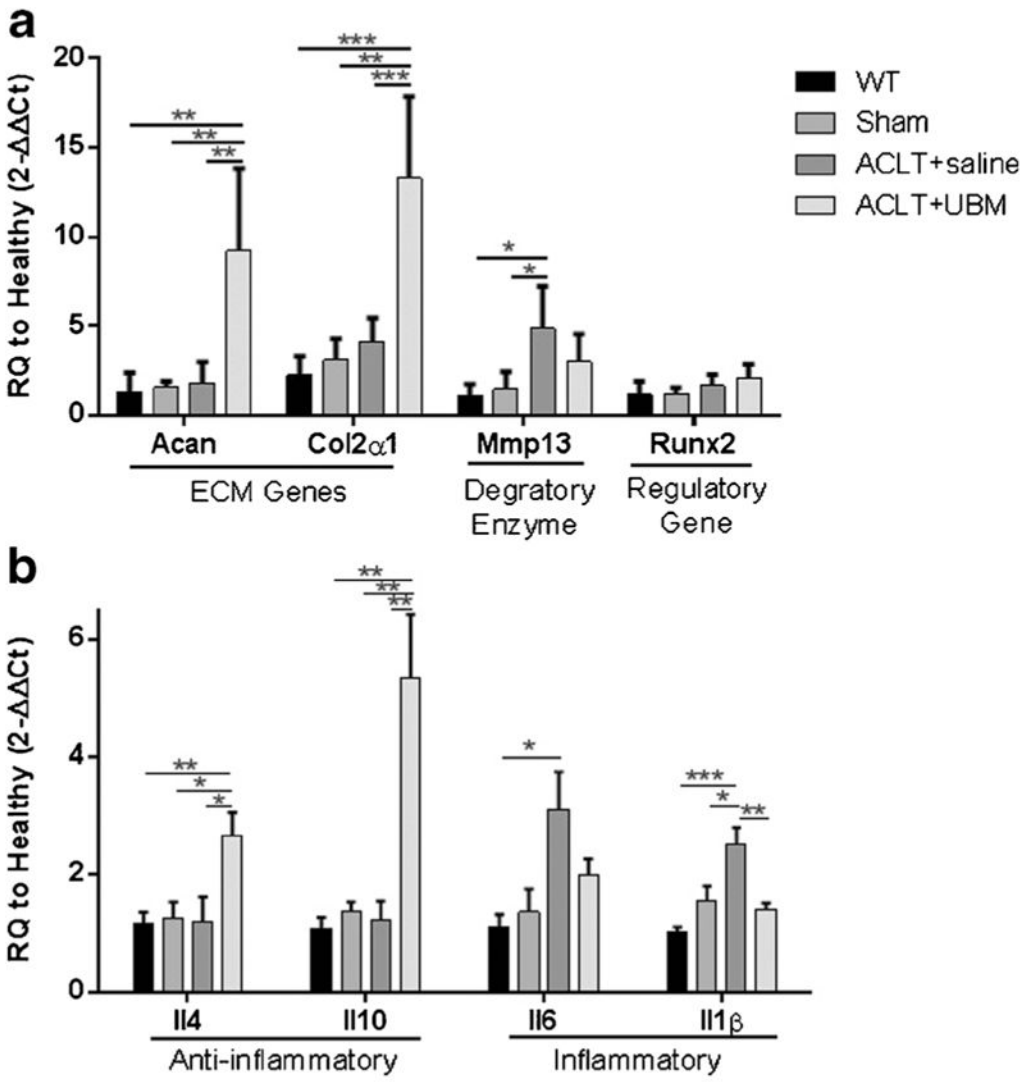

Fig. 2.

UBM injection decreases expression of inflammatory markers 4 weeks post-ACLT. Quantitative PCR on whole joint samples at 4 weeks post UBM injection. **a** Cartilage-related genes. UBM-treated mice increased Aggrecan (*Acan*) and Collagen 2α1 (*Col2a1*) expression compared to saline treatment. Additionally, expression of matrix metalloproteinase 13 (*Mmp13)* and RUNX2 (*Runx2*) is not statistically significantly increased over wild type. **b** Immune-related genes. UBM-treated mice increased IL-4 (*Il4*) and IL-10 (*Il10)* expression and decreased IL-1β (*Il1b*) expression compared to PBS control mice. Expression of interleukin-6 (*Il6*) is not statistically significantly increased over wild type. *$p < 0.05$, **$p < 0.01$, ***$p < 0.001$, ****$p < 0.0001$

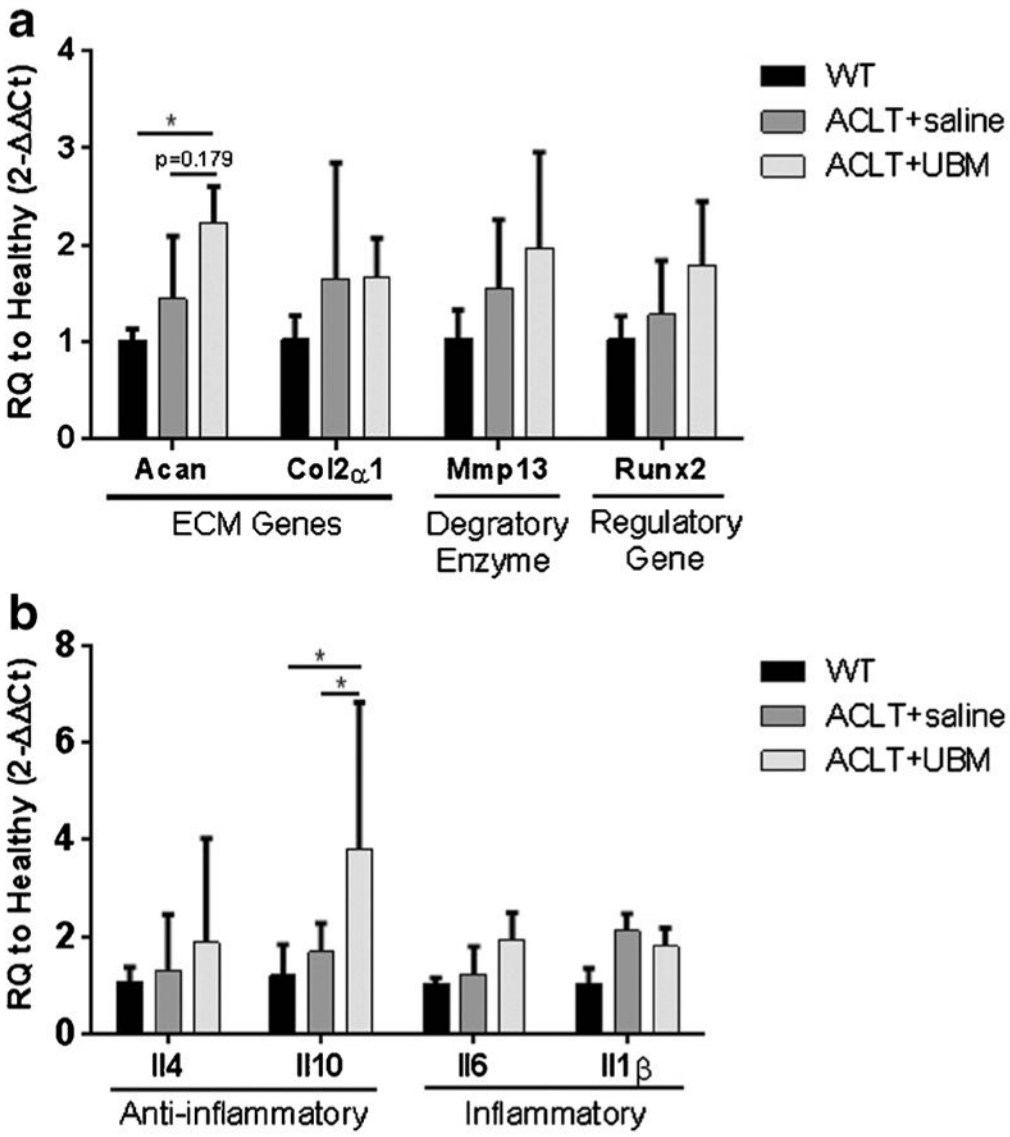

Fig. 3.

UBM injection decreases expression of inflammatory markers 8 weeks post-ACLT. Quantitative PCR on whole joint samples at 8 weeks post UBM injection. **a** Cartilage-related genes. UBM-treated mice increased Aggrecan (*Acan*) expression compared to WT treatment. **b** Immune-related genes. UBM-treated IL-10 (*Il10*) expression compared to PBS control mice. *$p < 0.05$, **$p < 0.01$, ***$p < 0.001$, ****$p < 0.0001$

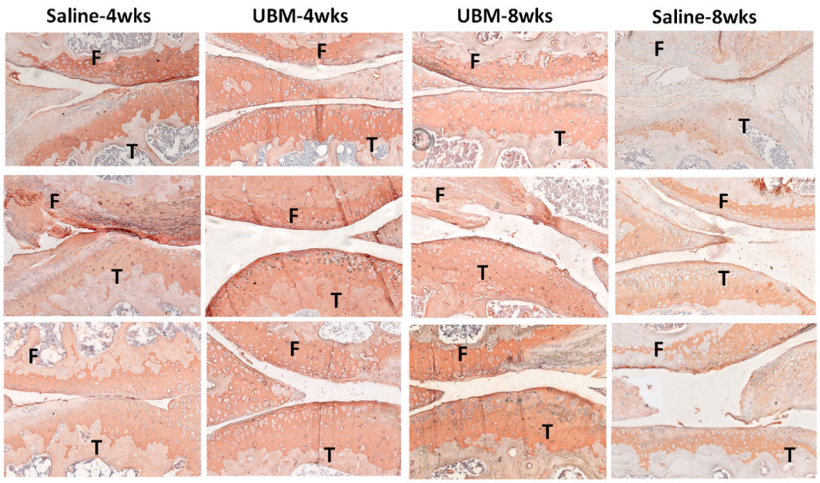

Fig. 4.

Collagen 2α1 staining. Slides close to the representative image used for OARSI scoring for each joint were stained with col2α1 to verify the PCR results of increased *col2α1* gene expression. Qualititatively, UBM-treated animals at 4 weeks post surgery have more intense col2α1 staining compared to the saline control group. The 8-week UBM group is improved compared to saline; however. it is not as intense as at 4 weeks. All slides were counterstained with hematoxylin. *F* = femur, *T* = tibia

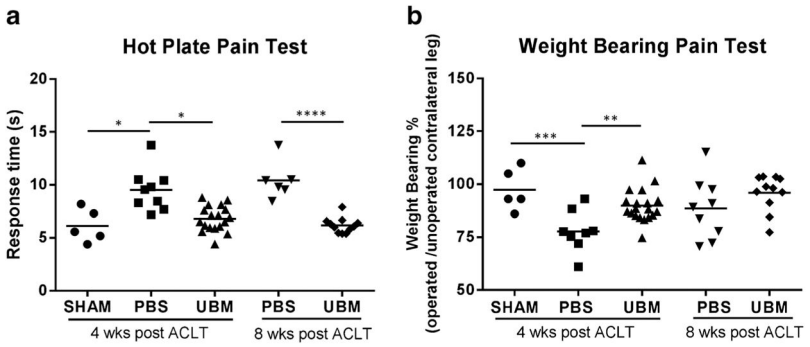

Fig. 5.

UBM treatment reduces pain. UBM-treated mice have reduced pain at 4 weeks compared to PBS control mice. **a** UBM-treated mice have reduced time on the hotplate compared to PBS control mice, indicating less pain in the operated leg. **b** UBM-treated mice have increased weight placed on the operated leg as measured by incapacitance testing, also indicating less pain on the operated leg. *$p < 0.05$, **$p < 0.01$, ***$p < 0.001$, ****$p < 0.0001$

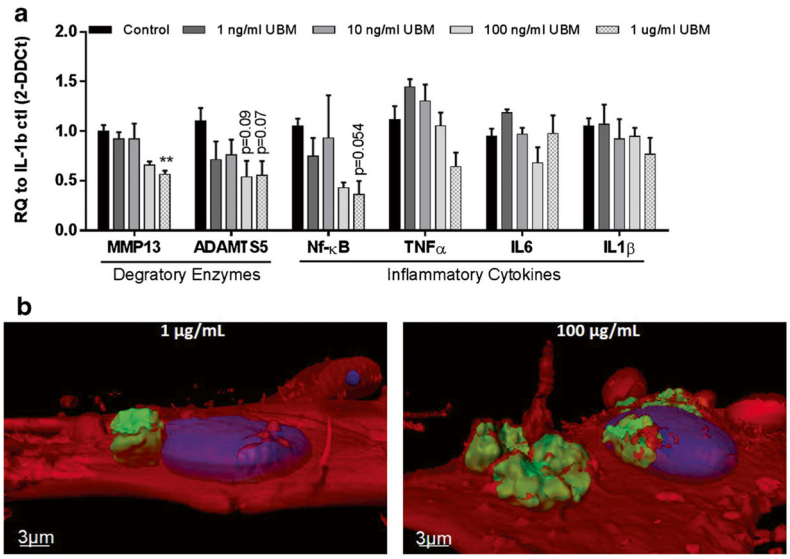

Fig. 6.

UBM decreased inflammatory markers in human primary chondrocytes **a** Gene expression data from *in vitro* human chondrocytes exposed to 10 ng/mL of IL-1β and 1 ng/mL–1 µg/mL of UBM ($n = 3$). *$p < 0.05$, **$p < 0.01$. **b** Confocal imaging of 1 µg/mL UBM (*left*) and 100 µg/mL UBM (*right*) 24 h after addition into cell culture medium. *Red* = cell membrane (seen at 50% transparency), *blue* = nucleus, *green* = UBM. UBM particles appear to be almost entirely encapsulated by the cell membrane after only 24 h